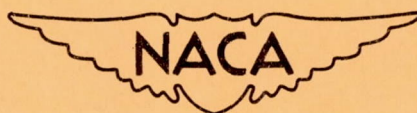# NATIONAL ADVISORY COMMITTEE FOR AERONAUTICS

TECHNICAL NOTE 3736

POISSON'S RATIOS AND VOLUME CHANGES FOR

PLASTICALLY ORTHOTROPIC MATERIAL

By Elbridge Z. Stowell and Richard A. Pride

Langley Aeronautical Laboratory
Langley Field, Va.

NACA

Washington

August 1956

NATIONAL ADVISORY COMMITTEE FOR AERONAUTICS

TECHNICAL NOTE 3736

POISSON'S RATIOS AND VOLUME CHANGES FOR

PLASTICALLY ORTHOTROPIC MATERIAL

By Elbridge Z. Stowell and Richard A. Pride

SUMMARY

Measurements of Poisson's ratios have been made in three orthogonal
directions on aluminum-alloy blocks in compression and on stainless-steel
sheet in both tension and compression. These measurements, as well as
those obtained by density determinations, show that there is no permanent
plastic change in volume within the accuracy of observation. A method is
suggested whereby a correlation may be effected between the measured indi-
vidual values of the Poisson's ratios and the stress-strain curves for the
material. Allowance must be made for the difference in the stress-strain
curves in tension and compression; this difference, wherever it appears,
is accompanied by significant changes in the Poisson's ratios.

INTRODUCTION

Probably there has never existed a block of metal in which all three
stress-strain curves in the principal directions were precisely identical.
Most metals, even if they appear to be isotropic in the elastic region,
hardly ever strain-harden to exactly the same degree in all directions.
The very process by which the block was fabricated almost always insures
that the properties in one direction will be different from the properties
in some other direction. This conclusion is borne out by recent tests on
six aircraft materials, all of which became anisotropic in the plastic
range (ref. 1). The result is that, even though Young's modulus and
Poisson's ratio may be independent of direction when the metal is stressed
elastically, anisotropy will appear when the metal is stressed plastically.
The effect of this anisotropy is to distort the behavior of the metal in
the plastic region from that predicted on the usual basis of isotropy.
The differences are not small; errors of 50 percent or more in strains
would not be uncommon when anisotropy is neglected.

Several investigators have made measurements of the Poisson's ratios
for aircraft materials in tension when stressed into the plastic range.
The six aircraft metals in sheet form studied in reference 1 all exhibited
anisotropy; that is, the Poisson's ratios varied with direction in the
plane of the sheet. The values ranged from a minimum of 0.222 for mag-
nesium to a maximum of 0.768 for commercially pure titanium.

Jackson, Smith, and Lankford (ref. 2) studied the anisotropy of sheet steel in the plastic range and measured the four Poisson's ratios associated with the two principal directions in the plane of the sheet. Their primary interest was in extension of the theory of plasticity to include the effects of anisotropy, but one of their conclusions was that the ratio of the two values of Poisson's ratio for each loading condition was a constant in the far plastic range.

The plastic anisotropy of thick 2024-T4 aluminum-alloy plate was studied by Klingler and Sachs (ref. 3). The plate was sufficiently thick $\left(1\frac{1}{2} \text{ inches}\right)$ so that stress-strain curves could be obtained from specimens cut in the thickness direction. The six Poisson's ratios associated with the three principal directions were measured. The conclusion was likewise reached that the ratio of the two Poisson's ratios for any one loading condition was a constant in the far plastic range. Klingler and Sachs called attention to the fact that the stress-strain curves differed comparatively little in the three principal directions; this condition indicated that stress-strain curves in themselves are not a reliable guide to the amount of anisotropy present.

McEvily and Hughes (ref. 4) have shown that Poisson's ratio in the plastic range can be computed from a knowledge of the crystallographic anisotropy and the slip systems present in the crystals. From an engineering point of view, it is more convenient to use, instead, the stress-strain curves for the material, which reflect the statistical effect of the crystallographic anisotropy.

These experimental studies, although yielding data of considerable interest, were not sufficient in themselves to provide the required correlation between the Poisson's ratios and the properties of the materials as shown by their stress-strain curves. The above considerations led the National Advisory Committee for Aeronautics to devise a series of measurements of Poisson's ratios which would be sufficiently complete to indicate the connection between the stress-strain curves in the principal directions and the amount of anisotropy as evidenced by the values of the Poisson's ratios. These tests included compression loading as well as tensile loading and were not confined to sheet materials. In this way it was hoped that enough information about the materials chosen, namely, 2024-T4 aluminum alloy and 301 stainless steel, could be obtained to overcome the deficiencies of the tests reported in the literature.

The present report gives the results of the tests and semiempirical formulas which connect the values of the Poisson's ratios with the stress-strain curves for the materials.

SYMBOLS

x,y,z	coordinate directions of orthotropy
ϵ	strain
σ	stress
E	Young's modulus
μ	Poisson's ratio in plastic range
ν	Poisson's ratio in elastic range
X,Y,Z	auxiliary functions defined in appendix
E_s	secant modulus

Subscripts:

c	compression
t	tension
x,y,z	on ϵ, σ, and E, symbols denote direction; on μ and ν, first subscript denotes loading direction and second subscript denotes transverse strain direction

EXPERIMENTAL PROCEDURE

When an experimental program to provide accurate data on plastic anisotropy was planned, specimens were required which would permit accurate longitudinal and transverse strain measurement in the elastic and small plastic strain region.

Six compression specimens (1 inch by 1 inch by 3 inches) were machined from $3\frac{1}{4}$ -inch-thick plate of 2024-T4 aluminum alloy. Duplicate specimens were taken with the 3-inch axis parallel to each of three principal directions: the direction of rolling for the plate hereafter is referred to by the subscript x; the direction perpendicular to the rolling direction but in the rolling plane is hereafter referred to by the subscript y; and the direction perpendicular to the rolling plane is hereafter referred to by the subscript z. Orientation was maintained by keeping the coordinate system of the original plate scribed on the faces of the specimens throughout all stages of machining. Six tension specimens, $\frac{1}{4}$ inch diameter by

$1\frac{3}{4}$ inches long in the test section with an overall length of 3 inches, were machined from the same 2024-T4 aluminum-alloy plate with the same orientation as the compression specimens.

Tension and compression specimens machined from type 301 stainless-steel sheet $\frac{1}{16}$ inch thick were of a different configuration. In the plane of the sheet, six rectangular compression specimens (2.52 inches long by 0.80 inch wide) were taken parallel to the x-axis and six parallel to the y-axis. These specimens were tested in a fixture which supported the sides against buckling. Two tensile specimens were machined from the flat sheet in the x-direction and two in the y-direction. These specimens were $\frac{1}{2}$ inch wide by $2\frac{1}{2}$ inches long in the test section with an overall length of $9\frac{3}{8}$ inches.

Forty-six rectangular pieces $\frac{7}{8}$ inch by 1 inch were machined from the stainless-steel sheet to be used in a stack test to determine the compression stress-strain curve in the z-direction. The flats of these pieces were rubbed lightly over No. 400 sandpaper to remove edge burrs and surface irregularities.

Special strain-measuring equipment employing linear variable-differential transformer-type gages was designed for these tests so that accurate direct measurement of strain in any direction could be made. Figure 1 shows a typical instrumentation for the aluminum-alloy compression blocks. Displacements in the direction of loading were picked up by two extensometers with knife edges. Displacements perpendicular to the direction of loading were picked up by two transverse extensometers with gage points. The extensometers were suspended in their proper positions and held against the specimen with light, elastic clamping forces.

Electrical output from the transformer units proportional to gage point displacement was amplified and fed into a multichannel recorder. Continuous records were obtained of load and individual strains simultaneously. This instrumentation permitted the recording of strain readings of 0.00001 inch per inch with errors of less than ±2 percent.

No attempt was made to measure the transverse strains on the $\frac{1}{4}$-inch-diameter aluminum tensile specimens. The displacements involved were too small to be measured with the same degree of accuracy as the compression test strains without a complete redesign of the strain-measuring equipment. However, strains in the direction of applied load were measured in the same way as in the compression tests and with comparable accuracy.

Instrumentation for the stainless-steel sheet specimens was similar to that for the aluminum-alloy compression tests. Figure 2 is a photograph of a

typical compression test on a sheet specimen. Longitudinal strains were
measured by the same knife-edge extensometers mounted on the edges of the
specimen which extend slightly beyond the side supports. Transverse dis-
placement was measured by a single gage-point extensometer also mounted
on the edges of the specimen. No attempt was made to measure the trans-
verse displacements in the z-direction because of their extremely small
magnitude.

Measurements comparable to those made in compression were also made
in tension on the stainless-steel sheet. Again no attempt was made to
measure the displacements in the z-direction.

Four knife-edge extensometers were used to measure strains in the
direction of loading on the stack compression test for the stainless-
steel sheet in the z-direction. A small initial load had to be placed
on the stack to hold it in place while the extensometers were mounted.
No transverse displacements were measured in either direction on the
stack. Loads were applied in standard hydraulic testing machines with
errors of less than ±0.50 percent.

The total volume of the aluminum-alloy compression specimens was
determined before and after testing in order to check on the amount, if
any, of plastic volume change. The volume determination was obtained
by weighing with a precision analytical balance. Weights of the test
specimens in air and submerged in distilled water were taken and correc-
tions were made for air temperature, water temperature, and weight of
supporting wire. Specimen weights in air were of the order of magnitude
of 140 grams and were determined on the balance to a least reading of
0.0001 gram. The accuracy of the balance was estimated to be approxi-
mately 0.0020 gram.

FORMULAS FOR THE SUMS OF THE POISSON'S RATIOS

Consider a block of metal which is isotropic in the elastic range
and thus in this range possesses a single elastic modulus E and a sin-
gle Poisson's ratio ν. When this block is stressed in some direction
(for example, the direction of x) by a stress σ_x in the plastic range,
the elastic modulus E becomes the secant modulus E_x, and the elastic
Poisson's ratio ν by virtue of the plastic anisotropy splits into two
plastic Poisson's ratios μ_{xy} and μ_{xz}. (The directions of x, y,
and z are taken to be the principal directions of orthotropy.)

The stress-strain relations which describe this situation are

$$\left.\begin{array}{c} \epsilon_x = \dfrac{\sigma_x}{E_x} \\[3mm] \epsilon_y = -\mu_{xy}\,\dfrac{\sigma_x}{E_x} \\[3mm] \epsilon_z = -\mu_{xz}\,\dfrac{\sigma_x}{E_x} \end{array}\right\} \qquad (1)$$

where ϵ_x, ϵ_y, and ϵ_z are the strains in the x-, y-, and z-directions. Addition of these equations gives

$$\epsilon_x + \epsilon_y + \epsilon_z = \left(1 - \mu_{xy} - \mu_{xz}\right)\frac{\sigma_x}{E_x} \qquad (2)$$

But $\epsilon_x + \epsilon_y + \epsilon_z$ is the change in volume, which is assumed to be always elastic, and

$$\epsilon_x + \epsilon_y + \epsilon_z = \frac{1 - 2\nu}{E}\,\sigma_x \qquad (3)$$

When the two expressions for volume change are equated, there results

$$\frac{\mu_{xy} + \mu_{xz}}{E_x} = \frac{1}{E_x} - \frac{1 - 2\nu}{E} \qquad (4a)$$

For loading in the y- or z-directions, two similar equations are obtained:

$$\frac{\mu_{yz} + \mu_{yx}}{E_y} = \frac{1}{E_y} - \frac{1 - 2\nu}{E} \qquad (4b)$$

$$\frac{\mu_{zx} + \mu_{zy}}{E_z} = \frac{1}{E_z} - \frac{1 - 2\nu}{E} \qquad (4c)$$

If the block should happen to remain isotropic when stressed into the plastic range $\mu_{xy} = \mu_{xz} = \mu$ and $E_x = E_y = E_z = E_s$; equation (4a) then becomes a formula for the computation of Poisson's ratio for an isotropic material and is

$$\mu = \frac{1}{2} - \left(\frac{1}{2} - \nu\right)\frac{E_s}{E} \qquad (5)$$

This formula has appeared in reference 5.

RESULTS AND DISCUSSION

Stress-Strain Curves

Figure 3 presents both compression and tension stress-strain curves for the three directions of loading on 2024-T4 aluminum-alloy plate. The curves represent the average of the two tests in each direction. Maximum stress deviation from average was less than 0.50 percent.

Compression and tension stress-strain curves for type 301 stainless-steel sheet are given in figure 4. The solid curves represent averages of six tests each in the x- and y-directions in compression and two tests each in the x- and y-directions in tension. Maximum stress deviation from average was less than 3 percent. In order to obtain the stress-strain curve in the z-direction, 46 pieces of the material were arranged in a stack. Even though the initial strains were widely different at different parts of the stack, the average strains gave an elastic modulus in the z-direction which differed from the elastic moduli in the x- and in the y-directions by only 2 percent. At larger strains, the strain distribution became uniform. Since the strains were measured over 16 pieces, it is felt that the resulting material is representative of the z-direction. The z-curve in tension was computed to accompany the z-curve in compression by a method described in the appendix.

Poisson's Ratio Measurements

The solid curves of figure 5 show the average of the experimental values of the six Poisson's ratios for the 2024-T4 aluminum-alloy blocks in compression. The first of the triple subscripts denotes the direction of loading; the second, the direction of transverse strain measurement; and the third, whether the loading was compression or tension. The solid curves of figure 6 show the average of the experimental values of the four Poisson's ratios in the plane of the 301 stainless-steel sheet. The dashed curves in figures 5 and 6 show values of Poisson's ratio computed by a method suggested in the appendix.

Measurements of Volume Change

The measurement of volume change as a result of plastic straining was made in two ways: by direct measurement with an analytical balance, and indirectly by a test of the validity of equations (4) which were derived on the basis of no volume change.

The direct measurements indicated a permanent change in volume within the accuracy of measurement (0.01 percent) and thus cannot be considered

as showing any positive change. These results confirm those of Smith
(ref. 6), who observed density changes in six metals following the appli-
cation of large compressive stress. The changes proved to be of the order
of a few hundredths of 1 percent, and duplicate tests sometimes resulted
in positive, and sometimes negative, changes. Permanent volume changes
were concluded to be negligibly small.

Figure 7 shows a comparison of experimental and calculated volume-
change functions for 2024-T4 aluminum-alloy blocks. The points represent
values of the left-hand side of equations (4), of which all quantities are
experimentally determined. The curves give values of the right-hand side
of equations (4), of which all quantities are computed from the stress-
strain curves and from the elastic constants. It may be concluded that
equations (4) hold with very high accuracy and that the underlying assump-
tion of no plastic volume change is strictly confirmed.

Discussion of Cross-Relations Among Ratios of

Poisson's Ratio to Modulus

Figure 8 shows the result of comparing the sum

$$\frac{\mu_{xyc}}{E_{xc}} + \frac{\mu_{xyt}}{E_{xt}}$$

with the sum

$$\frac{\mu_{yxc}}{E_{yc}} + \frac{\mu_{yxt}}{E_{yt}}$$

at the same stress. (Other criteria besides equality of stress are, of
course, possible.) It is seen that the two sums are nearly equal even
though the individual terms vary widely; that is,

$$\frac{\mu_{xyc}}{E_{xc}} + \frac{\mu_{xyt}}{E_{xt}} \approx \frac{\mu_{yxc}}{E_{yc}} + \frac{\mu_{yxt}}{E_{yt}}$$

A relation similar to the preceding relation is found in the linear theory
of elasticity for a material which is elastically orthotropic. If, for
example, the material possesses elastic moduli E_x and E_y in the x-
and y-directions with corresponding Poisson's ratios ν_{xy} and ν_{yx}, then

$$\frac{\nu_{xy}}{E_x} = \frac{\nu_{yx}}{E_y}$$

Because no distinction has been made between compression and tension, the equation contains only two terms instead of four as in the relation for the plastic case.

CONCLUSIONS

Measurements of Poisson's ratios have been made in three orthogonal directions on aluminum-alloy blocks in compression and on stainless-steel sheet in both tension and compression. From these measurements the following conclusions may be made:

1. There is no permanent change of volume in the metals tested after stressing into the plastic range.

2. For any one plane of orthotropy, for example, the xy-plane, the sum of the values of the ratio of Poisson's ratio to Young's modulus μ_{xy}/E_x in compression and in tension is equal to the sum of the values of the ratio of Poisson's ratio to Young's modulus μ_{yx}/E_y in compression and in tension. This equality represents an extension of a similar relation found for materials which are orthotropic in the elastic range.

3. The correlation of the values of the Poisson's ratios with the stress-strain curves as suggested in this paper will presumably be subject to future testing on these and on other materials. Such a correlation, however, appears to be possible.

Langley Aeronautical Laboratory,
    National Advisory Committee for Aeronautics,
        Langley Field, Va., April 26, 1956.

APPENDIX

SUGGESTED FORMULAS FOR POISSON'S RATIOS FOR A

PLASTICALLY ORTHOTROPIC MATERIAL

The results of figure 7 show that

$$\left.\begin{aligned}
\frac{\mu_{xy} + \mu_{xz}}{E_x} &= \frac{1}{E_x} - \frac{1 - 2\nu}{E} \\[2ex]
\frac{\mu_{yz} + \mu_{yx}}{E_y} &= \frac{1}{E_y} - \frac{1 - 2\nu}{E} \\[2ex]
\frac{\mu_{zx} + \mu_{zy}}{E_z} &= \frac{1}{E_z} - \frac{1 - 2\nu}{E}
\end{aligned}\right\} \tag{A1}$$

where E is the common elastic modulus, and E_x, E_y, and E_z are secant moduli in the x-, y-, and z-directions.

Furthermore, if the material properties differ in compression and in tension, figure 8 seems to indicate that, at the same stress,

$$\frac{\mu_{xyc}}{E_{xc}} + \frac{\mu_{xyt}}{E_{xt}} = \frac{\mu_{yxc}}{E_{yc}} + \frac{\mu_{yxt}}{E_{yt}} \tag{A2}$$

with similar equations for the yz-plane and for the xz-plane.

The assumption is made that, if, after loading in the x-direction, the value of μ_{xy} differs from the value of μ_{xz}, it is because the material properties in the y-direction are different from the properties in the z-direction. This assumption is given in analytical form as

$$\left.\begin{aligned}
\frac{\mu_{xy}}{E_x} &= \frac{1}{2E_x} - \frac{\frac{1}{2} - \nu}{E} + f\left(\frac{1}{E_y} - \frac{1}{E_z}\right) \\[2ex]
\frac{\mu_{xz}}{E_x} &= \frac{1}{2E_x} - \frac{\frac{1}{2} - \nu}{E} - f\left(\frac{1}{E_y} - \frac{1}{E_z}\right)
\end{aligned}\right\} \tag{A3}$$

where f is a functional symbol. The difference $\frac{1}{E_y} - \frac{1}{E_z}$ is a measure of the amount of orthotropy present.

When the properties in compression are different from those in tension, the preceding relations may be extended to take account of the difference in properties as follows:

$$\frac{\mu_{xyc}}{E_{xc}} = \frac{1}{2E_{xc}} - \frac{\frac{1}{2} - \nu}{E} + f\left(\frac{1}{E_{yt}} - \frac{1}{E_{zt}}\right)$$

$$\frac{\mu_{xzc}}{E_{xc}} = \frac{1}{2E_{xc}} - \frac{\frac{1}{2} - \nu}{E} - f\left(\frac{1}{E_{yt}} - \frac{1}{E_{zt}}\right)$$

$$\frac{\mu_{xyt}}{E_{xt}} = \frac{1}{2E_{xt}} - \frac{\frac{1}{2} - \nu}{E} + f\left(\frac{1}{E_{yc}} - \frac{1}{E_{zc}}\right)$$

$$\frac{\mu_{xzt}}{E_{xt}} = \frac{1}{2E_{xt}} - \frac{\frac{1}{2} - \nu}{E} - f\left(\frac{1}{E_{yc}} - \frac{1}{E_{zc}}\right)$$

$$(A4)$$

Eight similar relations may be written for loading in the y- and z-directions.

Substitution of expressions (A4) into equation (A2) gives for the xy-plane

$$\frac{\mu_{xyc}}{E_{xc}} + \frac{\mu_{xyt}}{E_{xt}} = \frac{1}{2}\left(\frac{1}{E_{xc}} + \frac{1}{E_{xt}}\right) - \frac{1 - 2\nu}{E} + f\left(\frac{1}{E_{yt}} - \frac{1}{E_{zt}}\right) + f\left(\frac{1}{E_{yc}} - \frac{1}{E_{zc}}\right) \quad (A5a)$$

Similarly,

$$\frac{\mu_{yxc}}{E_{yc}} + \frac{\mu_{yxt}}{E_{yt}} = \frac{1}{2}\left(\frac{1}{E_{yc}} + \frac{1}{E_{yt}}\right) - \frac{1 - 2\nu}{E} - f\left(\frac{1}{E_{zt}} - \frac{1}{E_{xt}}\right) - f\left(\frac{1}{E_{zc}} - \frac{1}{E_{xc}}\right) \quad (A5b)$$

for loading in the y-direction. These expressions will be equal provided

$$f(m) = \frac{m}{2}$$

where m represents any one of the four modulus differences.

When these values of the f-functions are introduced into equations (A3), the $\frac{\mu}{E}$ ratios take the form

$$\frac{\mu_{xyc}}{E_{xc}} = \frac{1}{2}\left(\frac{1}{E_{xc}} + \frac{1}{E_{yt}} - \frac{1}{E_{zt}}\right) - \frac{\frac{1}{2} - \nu}{E}$$

$$\frac{\mu_{xzc}}{E_{xc}} = \frac{1}{2}\left(\frac{1}{E_{xc}} - \frac{1}{E_{yt}} + \frac{1}{E_{zt}}\right) - \frac{\frac{1}{2} - \nu}{E}$$

$$\frac{\mu_{yzc}}{E_{yc}} = \frac{1}{2}\left(\frac{1}{E_{yc}} + \frac{1}{E_{zt}} - \frac{1}{E_{xt}}\right) - \frac{\frac{1}{2} - \nu}{E}$$

$$\frac{\mu_{yxc}}{E_{yc}} = \frac{1}{2}\left(\frac{1}{E_{yc}} - \frac{1}{E_{zt}} + \frac{1}{E_{xt}}\right) - \frac{\frac{1}{2} - \nu}{E}$$

$$\frac{\mu_{zxc}}{E_{zc}} = \frac{1}{2}\left(\frac{1}{E_{zc}} + \frac{1}{E_{xt}} - \frac{1}{E_{yt}}\right) - \frac{\frac{1}{2} - \nu}{E}$$

$$\frac{\mu_{zyc}}{E_{zc}} = \frac{1}{2}\left(\frac{1}{E_{zc}} - \frac{1}{E_{xt}} + \frac{1}{E_{yt}}\right) - \frac{\frac{1}{2} - \nu}{E}$$

$$\frac{\mu_{xyt}}{E_{xt}} = \frac{1}{2}\left(\frac{1}{E_{xt}} + \frac{1}{E_{yc}} - \frac{1}{E_{zc}}\right) - \frac{\frac{1}{2} - \nu}{E}$$

$$\frac{\mu_{xzt}}{E_{xt}} = \frac{1}{2}\left(\frac{1}{E_{xt}} - \frac{1}{E_{yc}} + \frac{1}{E_{zc}}\right) - \frac{\frac{1}{2} - \nu}{E}$$

$$\frac{\mu_{yzt}}{E_{yt}} = \frac{1}{2}\left(\frac{1}{E_{yt}} + \frac{1}{E_{zc}} - \frac{1}{E_{xc}}\right) - \frac{\frac{1}{2} - \nu}{E}$$

$$\frac{\mu_{yxt}}{E_{yt}} = \frac{1}{2}\left(\frac{1}{E_{yt}} - \frac{1}{E_{zc}} + \frac{1}{E_{xc}}\right) - \frac{\frac{1}{2} - \nu}{E}$$

$$\frac{\mu_{zxt}}{E_{zt}} = \frac{1}{2}\left(\frac{1}{E_{zt}} + \frac{1}{E_{xc}} - \frac{1}{E_{yc}}\right) - \frac{\frac{1}{2} - \nu}{E}$$

$$\frac{\mu_{zyt}}{E_{zt}} = \frac{1}{2}\left(\frac{1}{E_{zt}} - \frac{1}{E_{xc}} + \frac{1}{E_{yc}}\right) - \frac{\frac{1}{2} - \nu}{E}$$

(A6)

These formulas for the individual values of μ/E may now be compared with the values obtained from the tests. When this comparison is made, it is found that $\dfrac{\mu_{xyc}}{E_{xc}}$ and $\dfrac{\mu_{xzt}}{E_{xt}}$ are underestimated and $\dfrac{\mu_{xzc}}{E_{xc}}$

and $\dfrac{\mu_{xyt}}{E_{xt}}$ are overestimated by the same small amount X; $\dfrac{\mu_{yzc}}{E_{yc}}$ and $\dfrac{\mu_{yxt}}{E_{yt}}$

are underestimated and $\dfrac{\mu_{yxc}}{E_{yc}}$ and $\dfrac{\mu_{yzt}}{E_{yt}}$ are overestimated by the same

small amount Y; and $\dfrac{\mu_{zxc}}{E_{zc}}$ and $\dfrac{\mu_{zyt}}{E_{zt}}$ are underestimated and $\dfrac{\mu_{zyc}}{E_{zc}}$

and $\dfrac{\mu_{zxt}}{E_{zt}}$ are overestimated by the same small amount Z. Hence the true expressions for the μ/E ratios are probably of the form

$$
\begin{aligned}
\frac{\mu_{xyc}}{E_{xc}} &= \frac{1}{2}\left(\frac{1}{E_{xc}} + \frac{1}{E_{yt}} - \frac{1}{E_{zt}}\right) - \frac{\frac{1}{2} - \nu}{E} + X &
\frac{\mu_{xyt}}{E_{xt}} &= \frac{1}{2}\left(\frac{1}{E_{xt}} + \frac{1}{E_{yc}} - \frac{1}{E_{zc}}\right) - \frac{\frac{1}{2} - \nu}{E} - X \\[2mm]
\frac{\mu_{xzc}}{E_{xc}} &= \frac{1}{2}\left(\frac{1}{E_{xc}} - \frac{1}{E_{yt}} + \frac{1}{E_{zt}}\right) - \frac{\frac{1}{2} - \nu}{E} - X &
\frac{\mu_{xzt}}{E_{xt}} &= \frac{1}{2}\left(\frac{1}{E_{xt}} - \frac{1}{E_{yc}} + \frac{1}{E_{zc}}\right) - \frac{\frac{1}{2} - \nu}{E} + X \\[2mm]
\frac{\mu_{yzc}}{E_{yc}} &= \frac{1}{2}\left(\frac{1}{E_{yc}} + \frac{1}{E_{zt}} - \frac{1}{E_{xt}}\right) - \frac{\frac{1}{2} - \nu}{E} + Y &
\frac{\mu_{yzt}}{E_{yt}} &= \frac{1}{2}\left(\frac{1}{E_{yt}} + \frac{1}{E_{zc}} - \frac{1}{E_{xc}}\right) - \frac{\frac{1}{2} - \nu}{E} - Y \\[2mm]
\frac{\mu_{yxc}}{E_{yc}} &= \frac{1}{2}\left(\frac{1}{E_{yc}} - \frac{1}{E_{zt}} + \frac{1}{E_{xt}}\right) - \frac{\frac{1}{2} - \nu}{E} - Y &
\frac{\mu_{yxt}}{E_{yt}} &= \frac{1}{2}\left(\frac{1}{E_{yt}} - \frac{1}{E_{zc}} + \frac{1}{E_{xc}}\right) - \frac{\frac{1}{2} - \nu}{E} + Y \\[2mm]
\frac{\mu_{zxc}}{E_{zc}} &= \frac{1}{2}\left(\frac{1}{E_{zc}} + \frac{1}{E_{xt}} - \frac{1}{E_{yt}}\right) - \frac{\frac{1}{2} - \nu}{E} + Z &
\frac{\mu_{zxt}}{E_{zt}} &= \frac{1}{2}\left(\frac{1}{E_{zt}} + \frac{1}{E_{xc}} - \frac{1}{E_{yc}}\right) - \frac{\frac{1}{2} - \nu}{E} - Z \\[2mm]
\frac{\mu_{zyc}}{E_{zc}} &= \frac{1}{2}\left(\frac{1}{E_{zc}} - \frac{1}{E_{xt}} + \frac{1}{E_{yt}}\right) - \frac{\frac{1}{2} - \nu}{E} - Z &
\frac{\mu_{zyt}}{E_{zt}} &= \frac{1}{2}\left(\frac{1}{E_{zt}} - \frac{1}{E_{xc}} + \frac{1}{E_{yc}}\right) - \frac{\frac{1}{2} - \nu}{E} + Z
\end{aligned}
\qquad \text{(A7)}
$$

Equations (A1) and (A2) still hold for this modified set of relations, as will be discovered by inspection. Note that, from equations (A7),

$$\frac{\mu_{xyc}}{E_{xc}} + \frac{\mu_{xyt}}{E_{xt}} = \frac{\mu_{yxc}}{E_{yc}} + \frac{\mu_{yxt}}{E_{yt}} = \frac{1}{2}\left(\frac{1}{E_{xc}} + \frac{1}{E_{xt}} + \frac{1}{E_{yc}} + \frac{1}{E_{yt}} - \frac{1}{E_{zc}} - \frac{1}{E_{zt}}\right) - \frac{1 - 2\nu}{E}$$

This relation was used to compute the z-tension stress-strain curve for the stainless-steel sheet. Values of the left-hand side were obtained from figure 8 as the mean of the two curves. All the quantities on the right-hand side are known except $1/E_{zt}$, which could now be determined. From the values of $1/E_{zt}$, the z-tension curve in figure 4 was drawn.

In order to determine the correction terms X, Y, and Z, the following set of conditions may be imposed:

(a) The functions X, Y, and Z must involve differences of moduli, because each ratio must reduce to equation (5) when the material is isotropic.

(b) The functions must be symmetrical in tension and compression; otherwise, μ_{xyc}/E_{xc} could not be added to μ_{xyt}/E_{xt} to give the correct result.

(c) The functions are of the nature of correction terms and thus might be considered as arising from the difference between the stress-strain curves in compression and tension (Bauschinger effect). Thus, the functions might be expected to disappear in the absence of the Bauschinger effect.

(d) The functions should probably disappear at large strains.

For an x-loading, a function of the form

$$X \approx \frac{1}{E} \frac{\left(\dfrac{1}{E_{yc}} - \dfrac{1}{E_{yt}}\right) - \left(\dfrac{1}{E_{zc}} - \dfrac{1}{E_{zt}}\right)}{\dfrac{1}{E_{xc}} + \dfrac{1}{E_{xt}}}$$

is obtained. Trials of functions of this type showed that they gave the trend of the data correctly; indeed, if

$$X = \frac{2\nu}{E} \frac{\left(\dfrac{1}{E_{yc}} - \dfrac{1}{E_{yt}}\right) - \left(\dfrac{1}{E_{zc}} - \dfrac{1}{E_{zt}}\right)}{\dfrac{1}{E_{xc}} + \dfrac{1}{E_{xt}}}$$

$$Y = \frac{2\nu}{E} \frac{\left(\dfrac{1}{E_{zc}} - \dfrac{1}{E_{zt}}\right) - \left(\dfrac{1}{E_{xc}} - \dfrac{1}{E_{xt}}\right)}{\dfrac{1}{E_{yc}} + \dfrac{1}{E_{yt}}}$$

$$Z = \frac{2\nu}{E} \frac{\left(\dfrac{1}{E_{xc}} - \dfrac{1}{E_{xt}}\right) - \left(\dfrac{1}{E_{yc}} - \dfrac{1}{E_{yt}}\right)}{\dfrac{1}{E_{zc}} + \dfrac{1}{E_{zt}}}$$

and the Poisson's ratios for the aluminum-alloy blocks and for the stainless steel are computed from the stress-strain curves, the dashed curves in figures 5 and 6 are obtained. The trend of the experimental curves is fairly well duplicated. As more data on widely different materials accumulate, modifications of these formulas may be suggested by the data.

At large strains, the Poisson's ratios would be approximated by the formulas:

$$\mu_{xyc} = \frac{1}{2}\left(1 + \frac{E_{xc}}{E_{yt}} - \frac{E_{xc}}{E_{zt}}\right) \qquad \mu_{xyt} = \frac{1}{2}\left(1 + \frac{E_{xt}}{E_{yc}} - \frac{E_{xt}}{E_{zc}}\right)$$

$$\mu_{xzc} = \frac{1}{2}\left(1 - \frac{E_{xc}}{E_{yt}} + \frac{E_{xc}}{E_{zt}}\right) \qquad \mu_{xzt} = \frac{1}{2}\left(1 - \frac{E_{xt}}{E_{yc}} + \frac{E_{xt}}{E_{zc}}\right)$$

$$\mu_{yzc} = \frac{1}{2}\left(1 + \frac{E_{yc}}{E_{zt}} - \frac{E_{yc}}{E_{xt}}\right) \qquad \mu_{yzt} = \frac{1}{2}\left(1 + \frac{E_{yt}}{E_{zc}} - \frac{E_{yt}}{E_{xc}}\right)$$

$$\mu_{yxc} = \frac{1}{2}\left(1 - \frac{E_{yc}}{E_{zt}} + \frac{E_{yc}}{E_{xt}}\right) \qquad \mu_{yxt} = \frac{1}{2}\left(1 - \frac{E_{yt}}{E_{zc}} + \frac{E_{yt}}{E_{xc}}\right)$$

$$\mu_{zxc} = \frac{1}{2}\left(1 + \frac{E_{zc}}{E_{xt}} - \frac{E_{zc}}{E_{yt}}\right) \qquad \mu_{zxt} = \frac{1}{2}\left(1 + \frac{E_{zt}}{E_{xc}} - \frac{E_{zt}}{E_{yc}}\right)$$

$$\mu_{zyc} = \frac{1}{2}\left(1 - \frac{E_{zc}}{E_{xt}} + \frac{E_{zc}}{E_{yt}}\right) \qquad \mu_{zyt} = \frac{1}{2}\left(1 - \frac{E_{zt}}{E_{xc}} + \frac{E_{zt}}{E_{yc}}\right)$$

If the stress-strain curves are such that, for example, E_{xt}/E_{yc} and E_{xt}/E_{zc} tend to become constants at large strains, it is easy to see the reason that μ_{xyt}/μ_{xzt} would also become a constant at large strains as reported in references 2 and 3.

REFERENCES

1. Goodman, Stanley, and Russell, Stanton B.: Poisson's Ratio of Aircraft
   Sheet Materials for Large Strains. WADC Tech. Rep. No. 53-7 (Con-
   tract No. PO 33(038)51-4061), Wright Air Dev. Center, U.S. Air Force,
   Feb. 1953.

2. Jackson, L. R., Smith, K. F., and Lankford, W. T.: Plastic Flow in
   Anisotropic Sheet Steel. Tech. Pub. No. 2440, Am. Inst. Mining
   and Metallurgical Eng., Aug. 1948.

3. Klingler, L. J., and Sachs, G.: Plastic Flow Characteristics of
   Aluminum-Alloy Plate. Jour. Aero. Sci., vol. 15, no. 10, Oct. 1948,
   pp. 599-604.

4. McEvily, Arthur J., Jr., and Hughes, Philip J.: An Experimental and
   Theoretical Investigation of the Anisotropy of 3S Aluminum-Alloy
   Sheet in the Plastic Range. NACA TN 3248, 1954.

5. Nádai, A.: Theory of Flow and Fracture of Solids. Vol. 1, second ed.,
   McGraw-Hill Book Co., Inc., 1950.

6. Smith, T. F. W.: Lateral-Longitudinal Strain Ratio for Plastic Strains.
   The Engineer, vol. 198, no. 5156, Nov. 19, 1954, pp. 692-693.
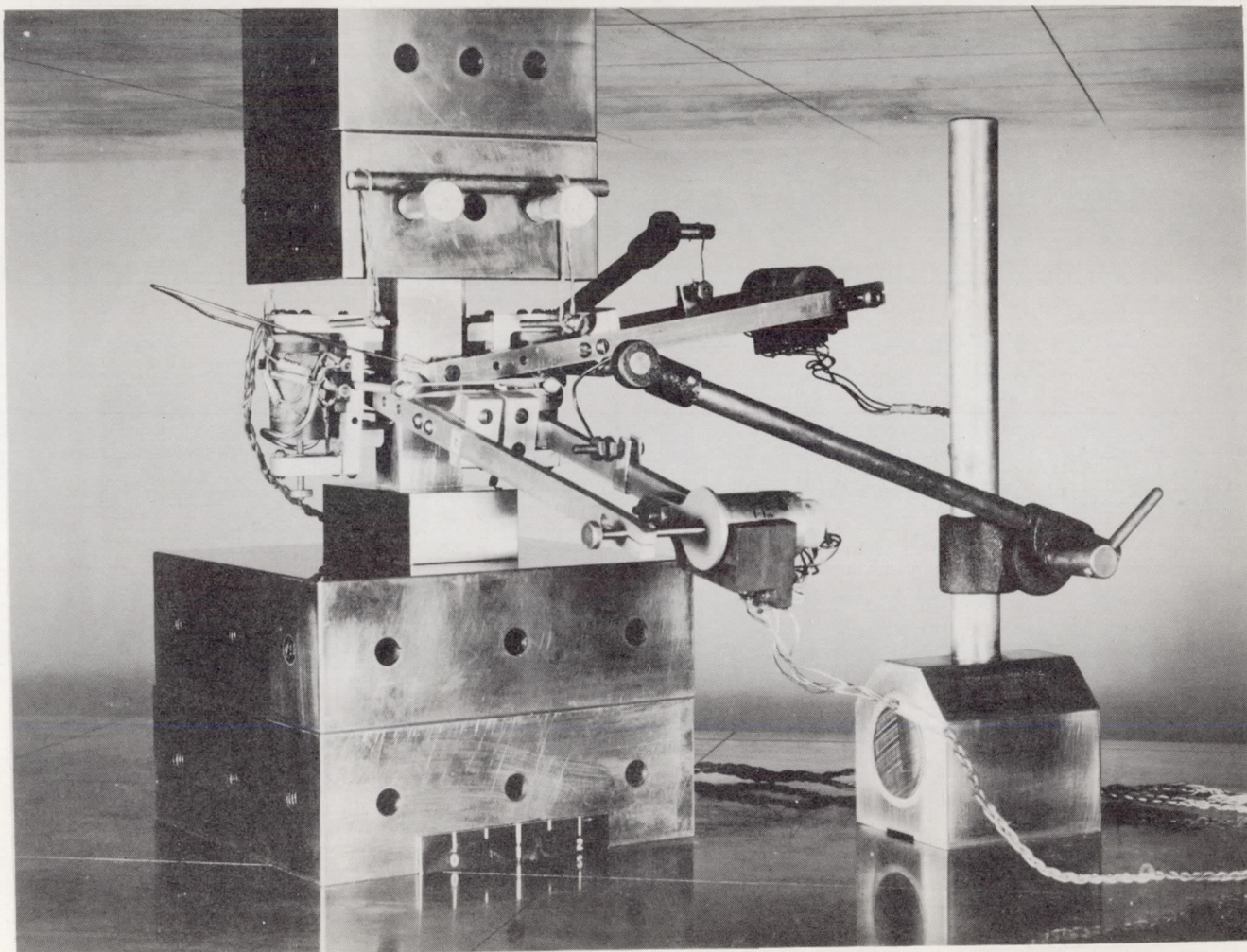
L-81857

Figure 1.- Instrumentation for obtaining Poisson's ratios on solid blocks
in compression.
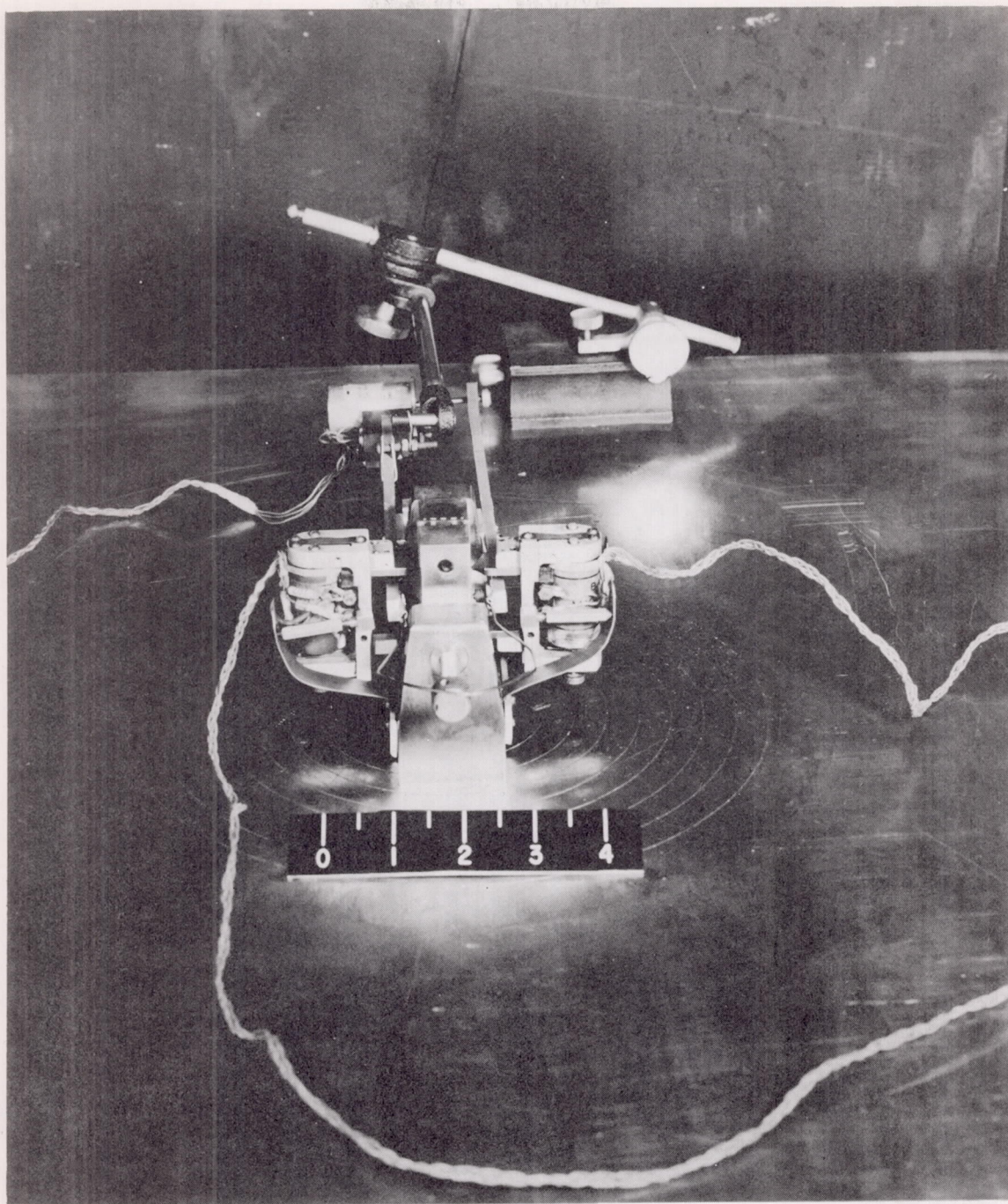
L-80892

Figure 2.- Instrumentation for obtaining Poisson's ratios on sheet materials
in compression.
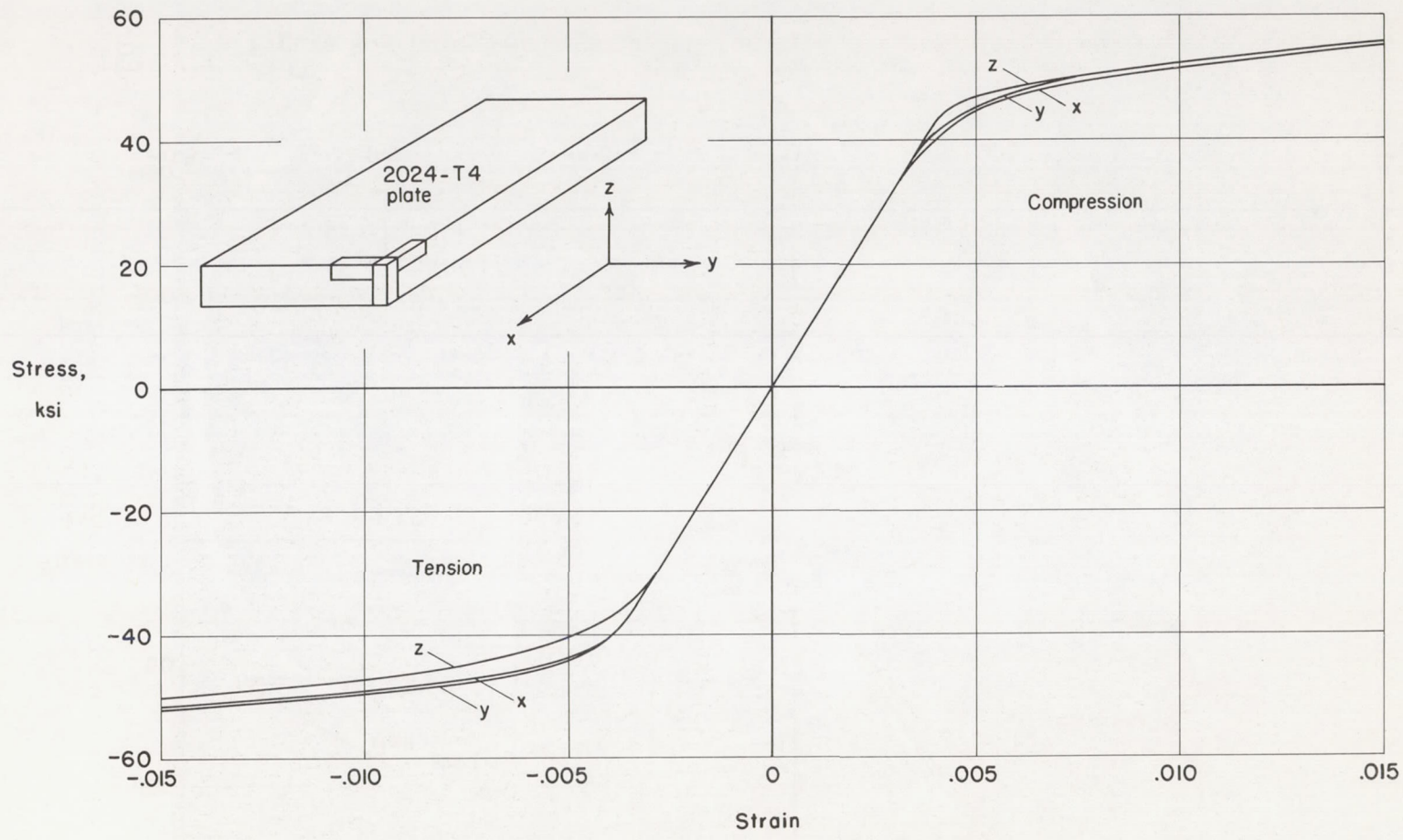
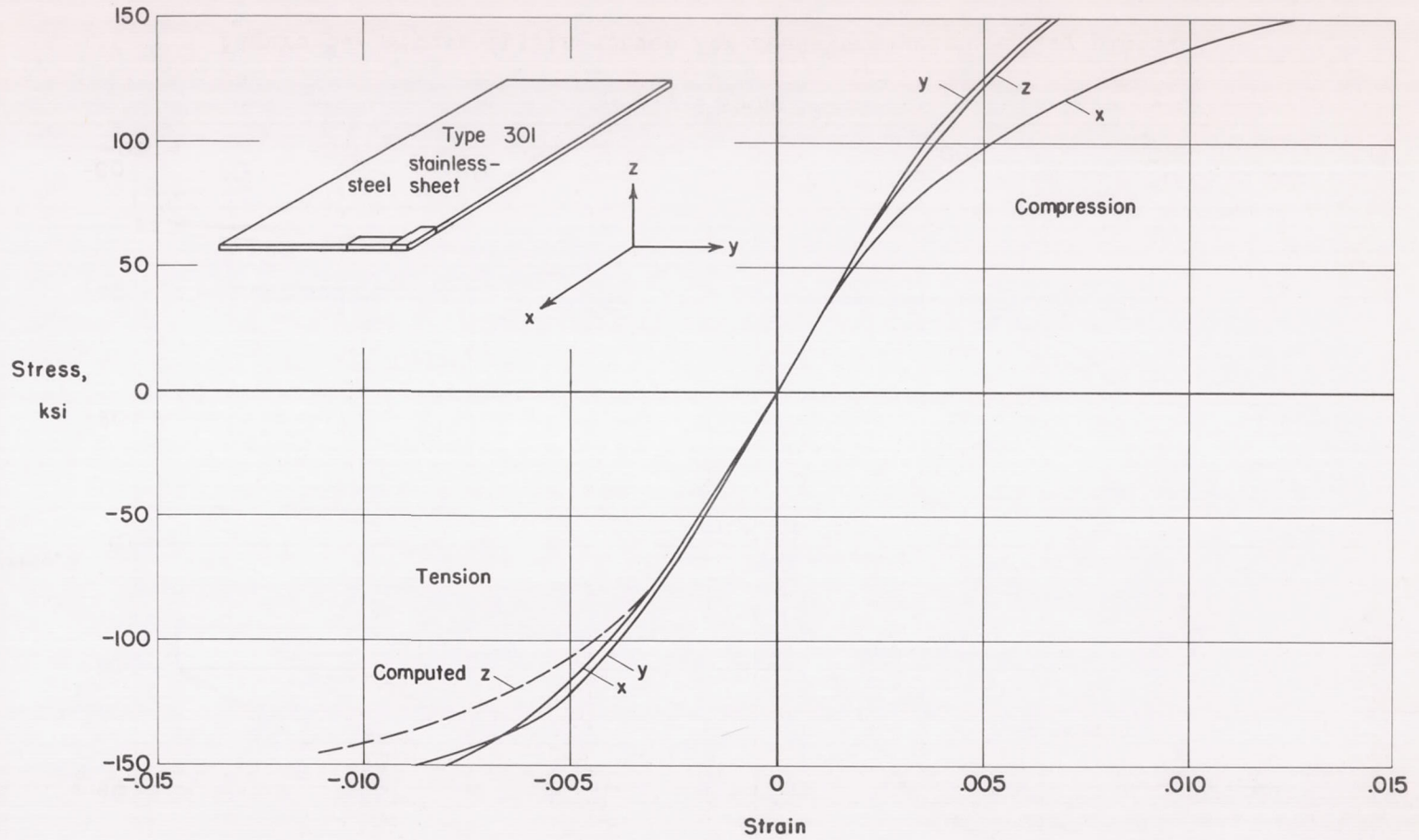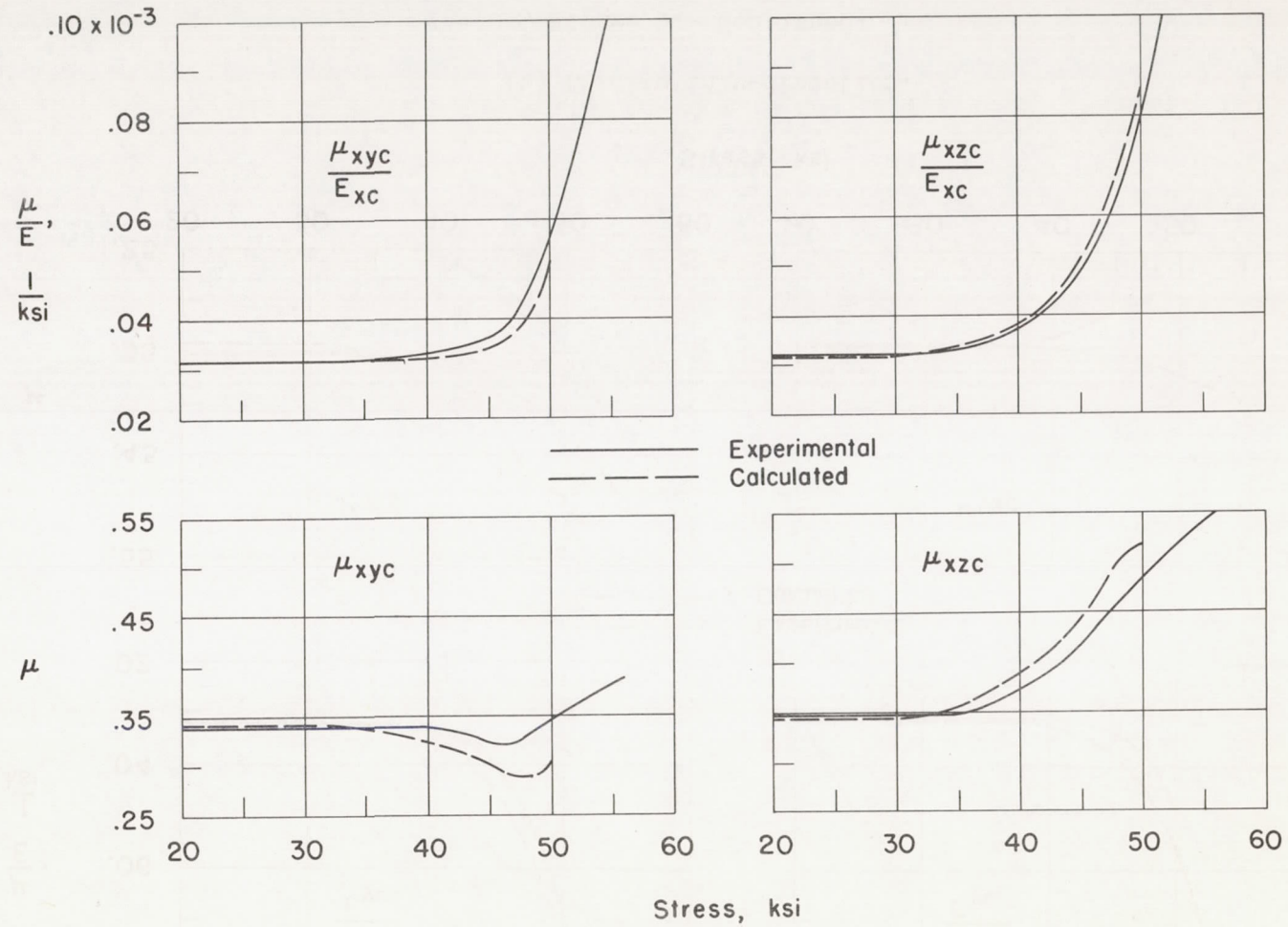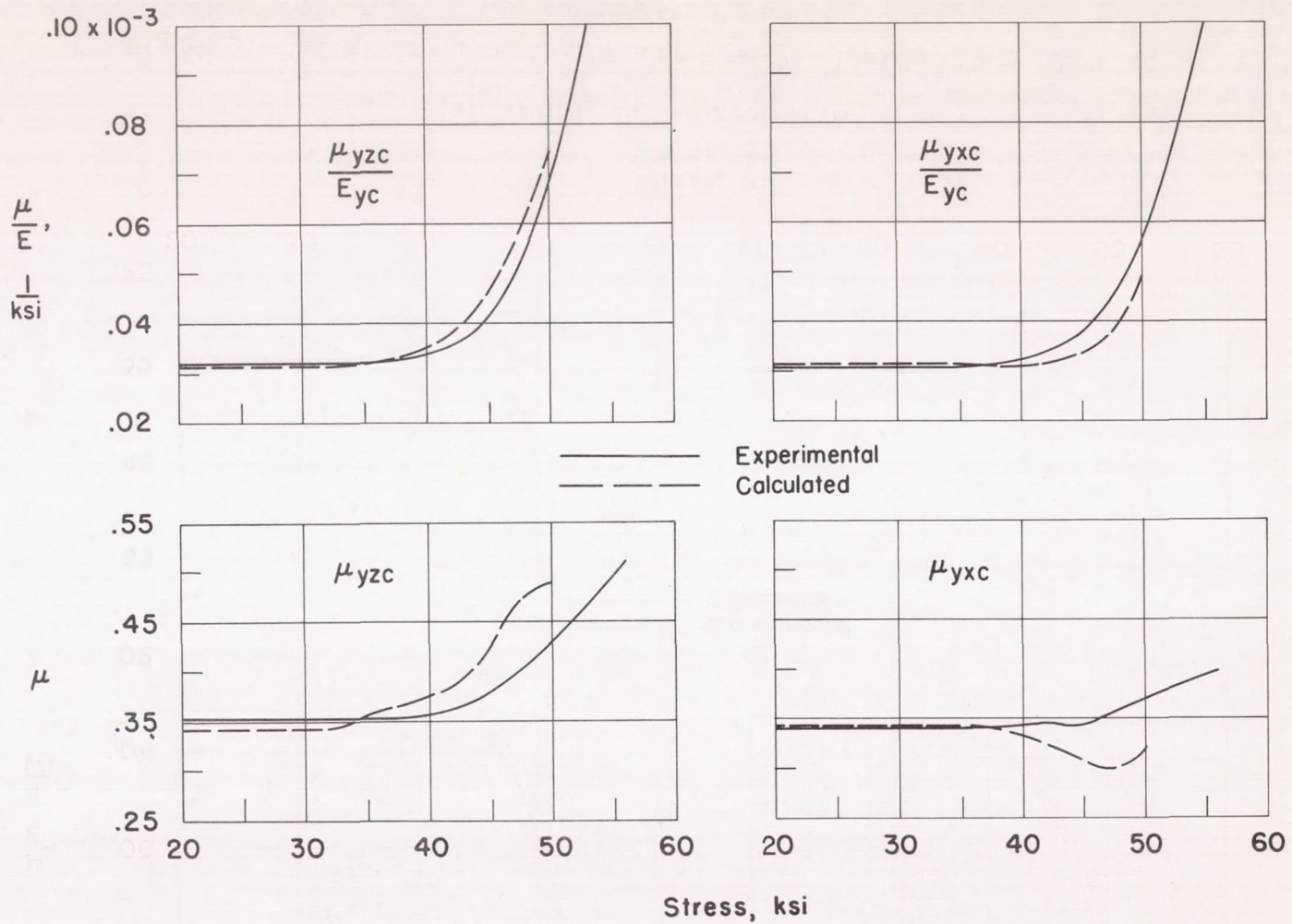Figure 3.- Stress-strain curves for 2024-T4 aluminum-alloy plate.

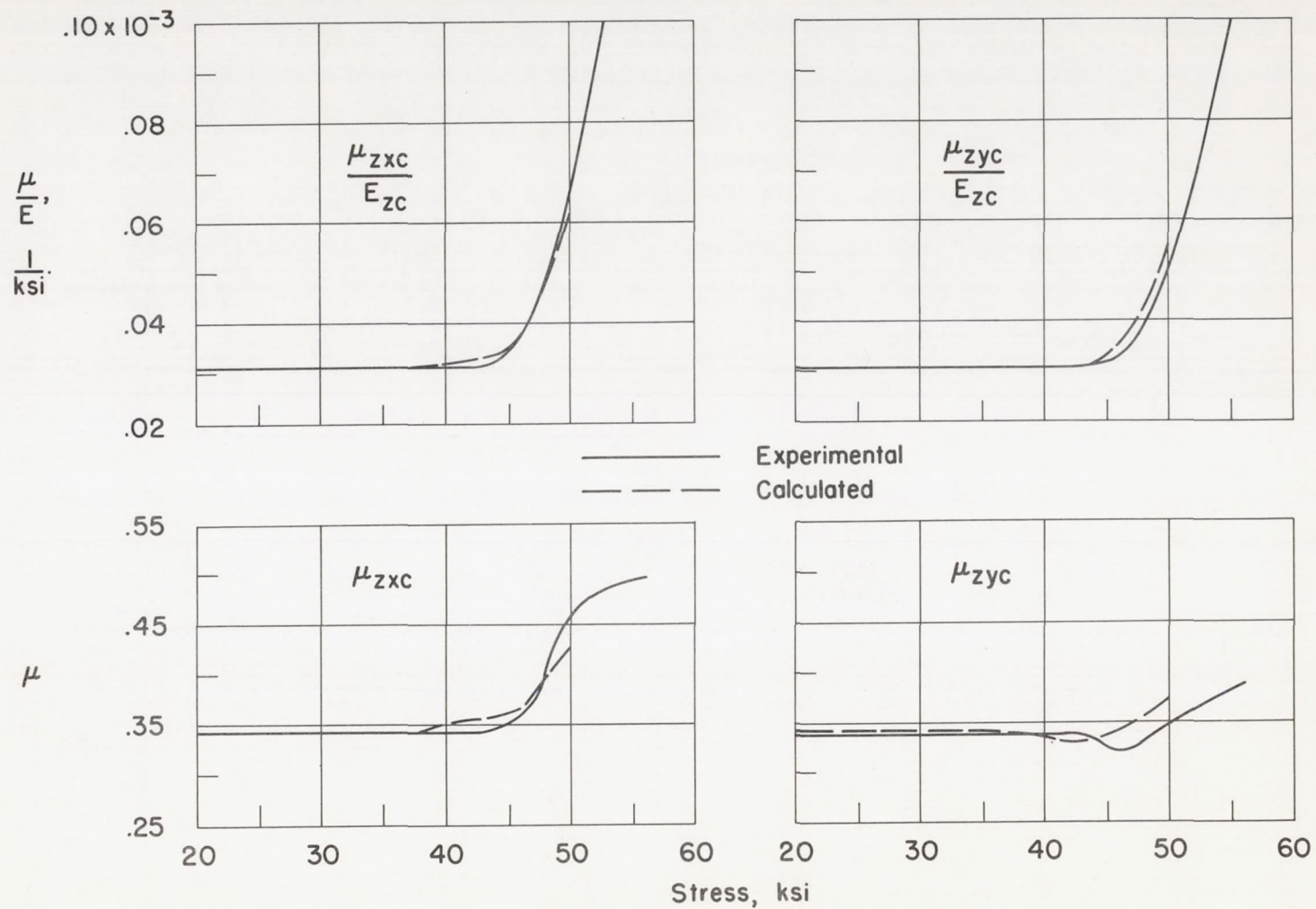Figure 4.- Stress-strain curves for type 301 stainless-steel sheet.

(a) Loading in x-direction.

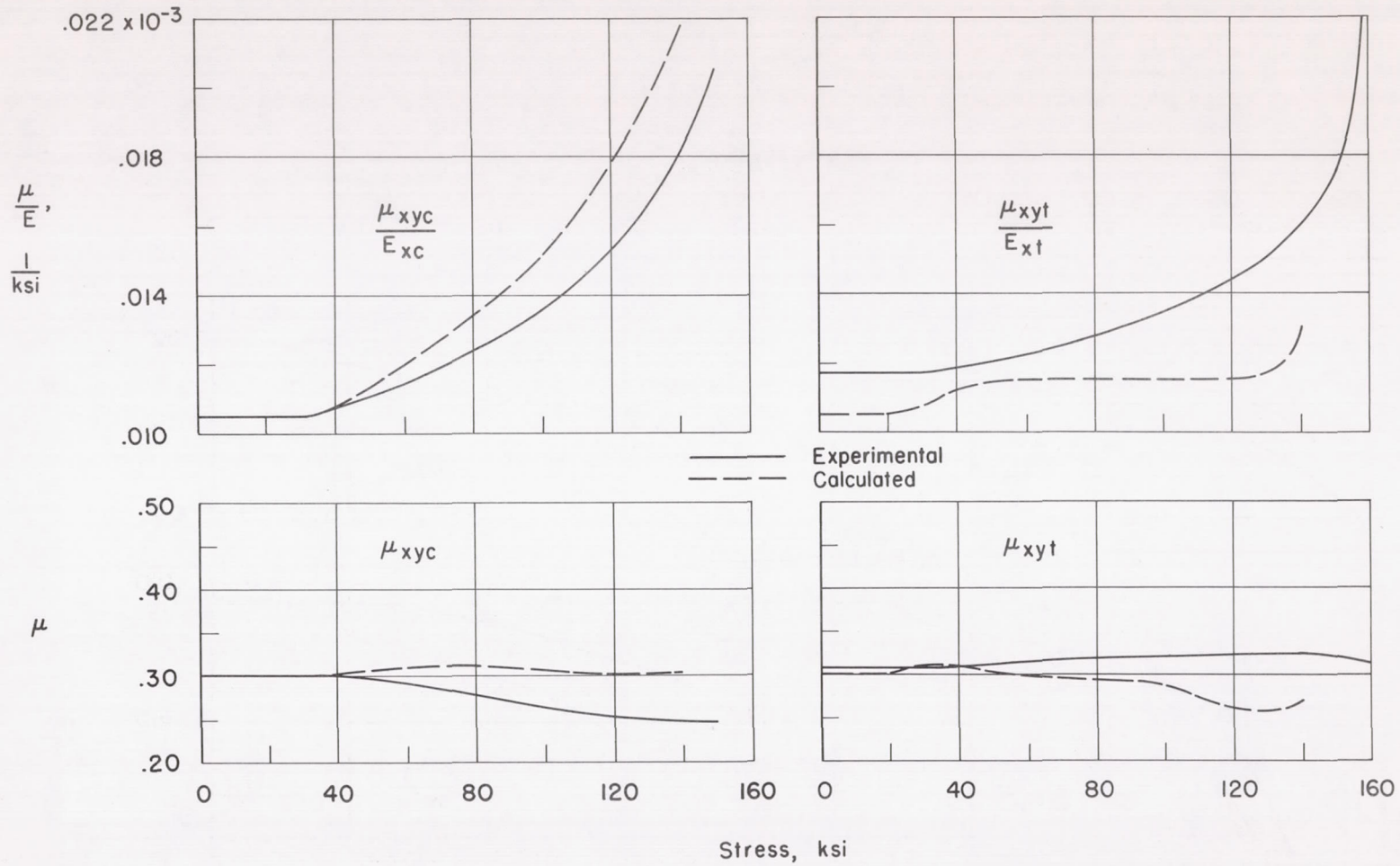Figure 5.- Values of μ and μ/E for 2024-T4 aluminum-alloy plate in compression.

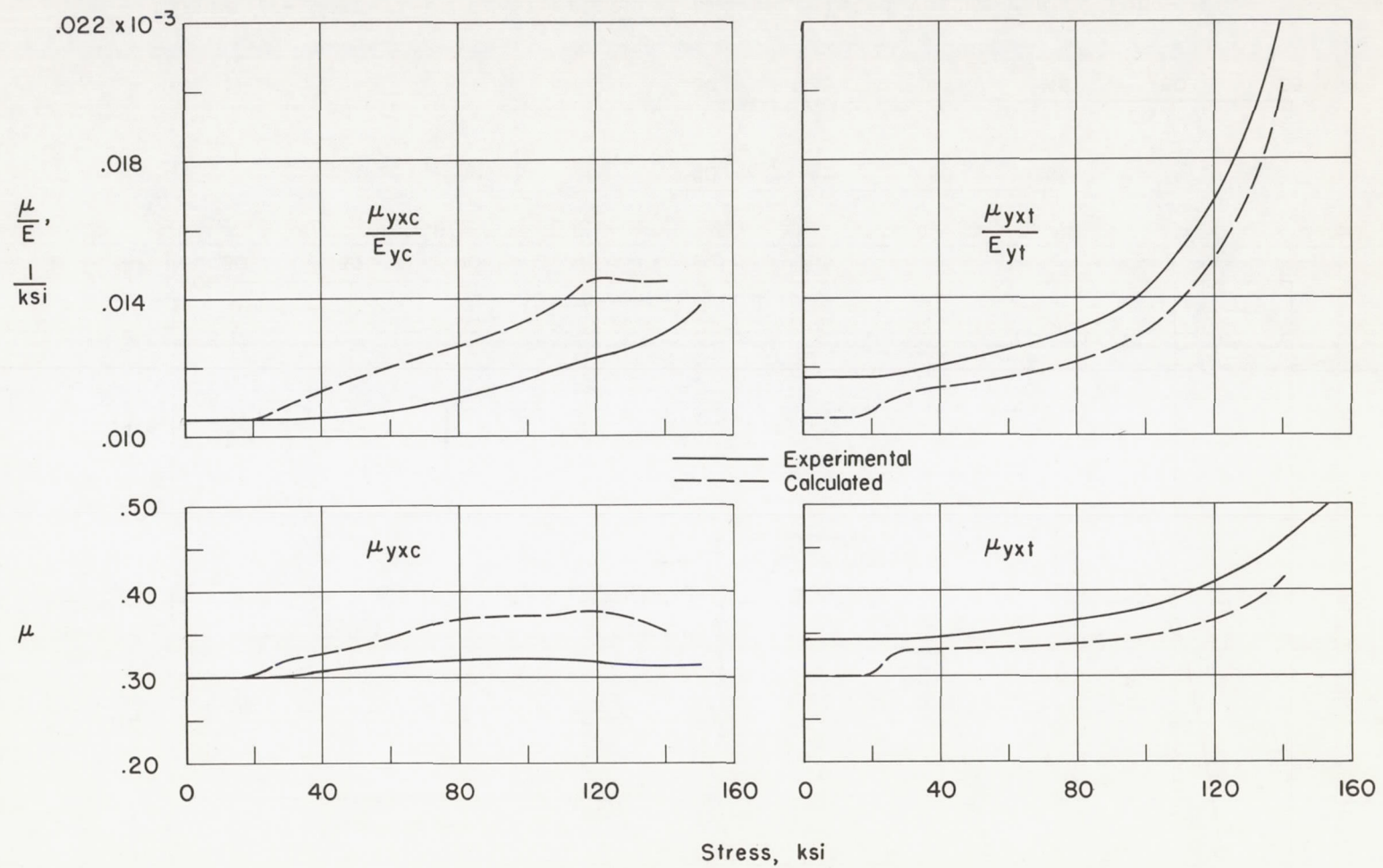(b) Loading in y-direction.

Figure 5.- Continued.

(c) Loading in z-direction.

Figure 5.- Concluded.

(a) Loading in x-direction.

Figure 6.- Values of μ and μ/E in the rolling plane of type 301
stainless-steel sheet for compression and tension loading.

$\dfrac{\mu}{E},$

$\dfrac{1}{ksi}$

$\dfrac{\mu_{yxc}}{E_{yc}}$

$\dfrac{\mu_{yxt}}{E_{yt}}$

Experimental

Calculated

μ

μ_{yxc}

μ_{yxt}

Stress, ksi

(b) Loading in y-direction.

Figure 6.- Concluded.

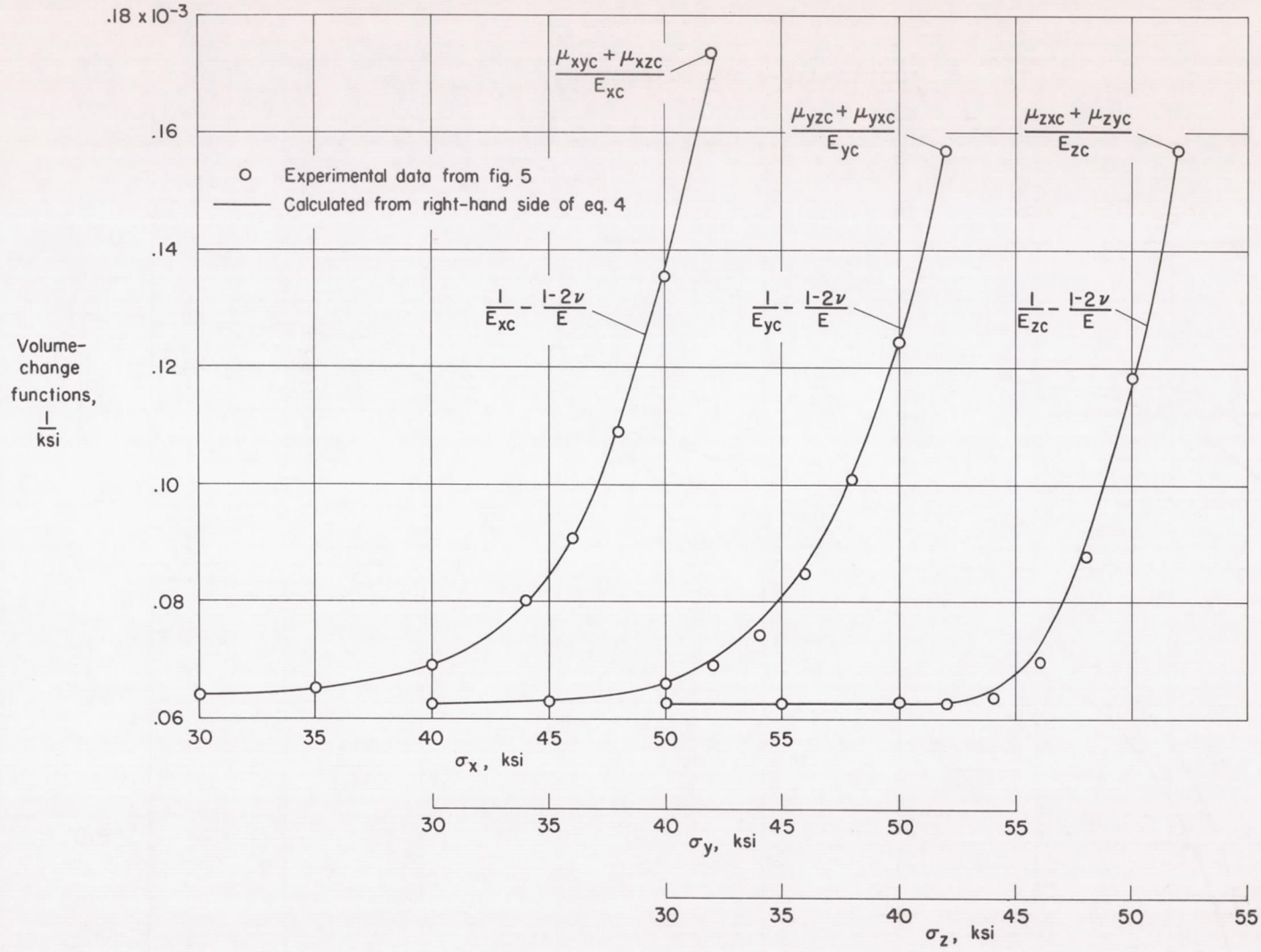Figure 7.- Comparison of experimental and calculated volume-change functions for 2024-T4 aluminum-alloy blocks.
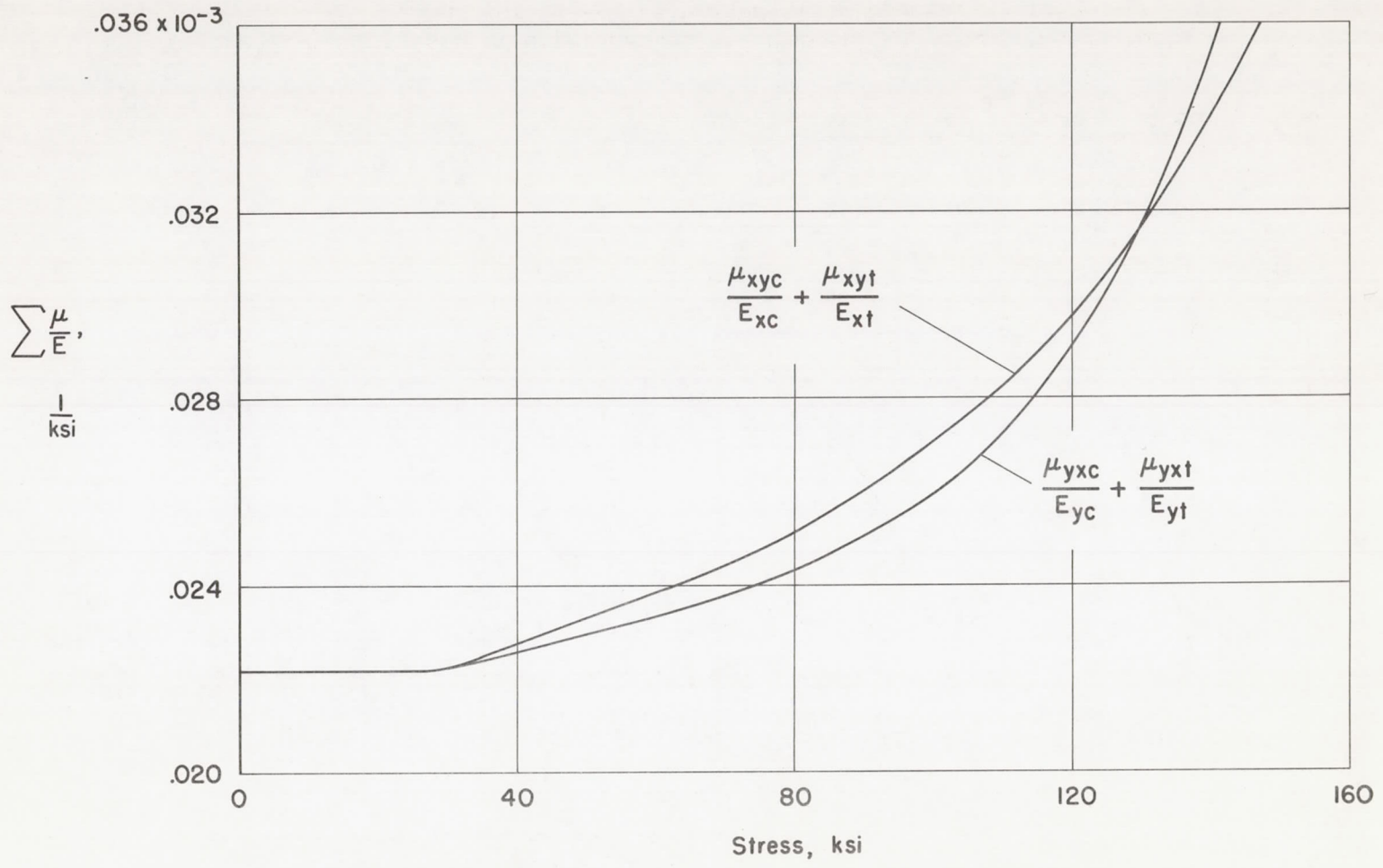
Figure 8.- Comparison of sums of μ/E for tension and compression of x-loading and y-loading with type 301 stainless-steel sheet. Individual values of μ/E from figure 6.